

Isabella L. Karle<sup>1</sup>  
Chittaranjan Das<sup>2</sup>  
P. Balaram<sup>2</sup>

<sup>1</sup> Laboratory for the Structure  
of Matter,  
Naval Research Laboratory,  
Washington, DC,  
20375-5341, USA

<sup>2</sup> Molecular Biophysics Unit,  
Indian Institute of Science,  
Bangalore-560 012, India

Received 27 December 2000;  
accepted 1 March 2001

## Effects of Hydrogen-Bond Deletion on Peptide Helices: Structural Characterization of Depsipeptides Containing Lactic Acid\*

**Abstract:** The insertion of  $\alpha$ -hydroxy acids into peptide chains provides a convenient means for investigating the effects of hydrogen bond deletion on polypeptide secondary structures. The crystal structures of three oligopeptides containing L-lactic acid (Lac) residue have been determined. Peptide **1**, Boc-Val-Ala-Leu-Aib-Val-Lac-Leu-Aib-Val-Ala-Leu-OMe (Boc: tert-butyloxycarbonyl; Aib:  $\alpha$ -aminoisobutyric acid; OMe: methyl ester), and peptide **2**, Boc-Val-Ala-Leu-Aib-Val-Lac-Leu-Aib-Val-Leu-OMe, adopt completely helical conformations in the crystalline state with the Lac(6) residue comfortably accommodated in the center of a helix. The distance between the O atoms of Leu(3) CO group and the Lac(6) O (ester) in both the structures is 3.1–3.3 Å. The NMR and CD studies of peptide **1** and its all-amide analogue **4**, Boc-Val-Ala-Leu-Aib-Val-Ala-Leu-Aib-Val-Ala-Leu-OMe, provide firm evidence for a continuous helical conformation in solution in both the cases. In a 14-residue peptide **3**, Boc-Val-Ala-Leu-Aib-Val-Ala-Leu-Val-Ala-Leu-Aib-Val-Lac-Leu-OMe, residues Val(1)–Leu(10) adopt a helical conformation. Aib(11) is the site of chiral reversal resulting in helix termination by formation of a Schellman motif. Residues 12–14 adopt nonhelical conformations. The loss of the hydrogen bond near the C-terminus appears to facilitate the chiral reversal at Aib(11). © 2001 John Wiley & Sons, Inc.† Biopolymers 59: 276–289, 2001

**Keywords:** 14-residue peptides; helix reversal; helix termination; Lac contained in helical backbone; x-ray crystal structures

## INTRODUCTION

Hydrogen bonds are ubiquitous in protein and peptide structures.<sup>1–5</sup> Historically, Pauling's formulation of

the  $\alpha$ -helical and  $\beta$ -sheet structures of polypeptides was based on the necessity of optimizing interactions between the CO and the NH groups in peptide backbones.<sup>6,7</sup> After the experimental observation of

Correspondence to: Isabella L. Karle or P. Balaram  
Contract grant sponsor: Department of Biotechnology, Government of India, National Institutes of Health, and the Office of Naval Research, Washington, DC

Contract grant sponsor: GM30902

\* In this article, all chiral amino acids are of the L configuration.  
Biopolymers, Vol. 59, 276–289 (2001)

© 2001 John Wiley & Sons, Inc. † This article is a US Government work and, as such, is in the public domain in the United States of America.

$\beta$ -bends in peptide structures,<sup>8–10</sup> studies that aimed to delineate all the stereochemically allowed conformations of a system of a three-linked peptide unit that possessed a 4  $\rightarrow$  1 hydrogen bond were published.<sup>11,12</sup> Although the importance of hydrogen bonds as a stabilizing interaction has long been recognized in chemistry and biology,<sup>13</sup> many recent discussions have centered on the precise contributions made by the backbone hydrogen bonds to the overall folded state of proteins.<sup>14–16</sup> As an extension of our studies on peptide helices, we have undertaken the synthesis and molecular characterization of sequences which contain appropriately positioned L-lactic acid (Lac) residues, permitting the insertion of an ester linkage into a polypeptide chain. The replacement of a hydrogen-bond donating NH group by an oxygen atom allows the selective removal of a specific hydrogen bond in the lactic acid containing analogue depsipeptides. Since the ester and the amide groups are approximately isosteric, no major structural perturbations unrelated to the hydrogen bond are expected<sup>17</sup> (Ramachandran conformational energy plots of L-alanine and L-lactic acid are very similar.<sup>18</sup>) The introduction of lactic acids and other  $\alpha$ -hydroxy acid analogues of amino acids into peptides has previously been investigated with respect to  $\beta$ -turn models,<sup>19,20</sup> depsipeptide analogues of elastin repeating sequences,<sup>21</sup> sequential peptide polymers with protected polar side chains,<sup>22,23</sup> and more recently in investigating potential minimal  $\beta$ -hairpins.<sup>24–26</sup>  $\alpha$ -Hydroxy acids have been introduced using the procedures developed for unnatural amino acid mutagenesis<sup>27</sup> into the proteins staphylococcal nuclease<sup>28,29</sup> and T4 lysozyme<sup>30</sup> in order to estimate hydrogen bond contributions to  $\beta$ -turn,  $\beta$ -sheet, and  $\alpha$ -helix stability. Semi-synthesis of a bovine pancreatic trypsin inhibitor (BPTI) analogue containing an ester bond in the backbone has been achieved.<sup>31</sup> Total chemical synthesis has been used to engineer ester linkages into the turkey ovomucoid third domain protease inhibitor in order to probe intermolecular main chain hydrogen bonding in serine proteinase-inhibitor complexes.<sup>32</sup> In the present study, we describe the structural characterization of peptide helices in which a single L-Lac residue has been positioned at the center of the helix or near the C-terminus. The crystal structures of three peptides containing Lac residues have been determined. Peptides **1** (Boc-Val-Ala-Leu-Aib-Val-Lac-Leu-Aib-Val-Ala-Leu-OMe; (Boc: *tert*-butyloxycarbonyl; Aib:  $\alpha$ -aminoisobutyric acid; OMe: methyl ester) and **3** (Boc-Val-Ala-Leu-Aib-Val-Ala-Leu-Val-Ala-Leu-Aib-Val-Lac-Leu-OMe) were designed in order to examine the effects of positioning of the hydroxy acid in the center of a helical sequence and toward the C-terminal end. Pep-

ptide **2** (Boc-Val-Ala-Leu-Aib-Val-Lac-Leu-Aib-Val-Leu-OMe), which was serendipitously obtained as a deletion sequence during synthesis, also yielded a crystal structure providing a second example of a hydroxy acid in the center of helical segment. The choice of peptide sequences was based on the well established tendency of the Aib residue to promote helix formation and enhance crystallinity in apolar sequences.<sup>33–38</sup> The robustness of  $3_{10}/\alpha$ -helical structures in heteromeric sequences containing Aib contents of 15–30% in variable positions has been extensively demonstrated by crystal structure analysis.<sup>33–35</sup>

## EXPERIMENTAL

### Peptide Synthesis

Peptides **1**, **3**, and **4** were synthesized by conventional solution phase methods<sup>39</sup> by using a fragment condensation strategy. During the assembly of **1**, peptide **2** was isolated as a synthetic side product with a deletion of the C-terminal Ala from **1**. The Boc group was used for N-terminal protection, and the C-terminus was protected as a methyl (OMe) or a benzyl ester (OBzl) functional group. Deprotections were performed using 98% formic acid or saponification for N- and C-terminus, respectively. The fragments containing lactic acid were subjected to catalytic hydrogenolysis to remove the benzyl ester protection from the C-terminus. Couplings were mediated by dicyclohexylcarbodiimide/1-hydroxybenzotriazole (DCC/HOBT), and in the cases of coupling involving the hydroxy group of lactic acid (for ester formation) DCC and dimethylaminopyridine (DMAP) were employed.<sup>40</sup> All the intermediates were characterized by <sup>1</sup>H NMR (80 MHz) and thin layer chromatography (TLC) on silica gel and used without further purification. The final peptides were purified by reverse phase, medium pressure liquid chromatography (MPLC) (C<sub>18</sub>, 40–60  $\mu$ ) and by high performance liquid chromatography (HPLC) on a reverse phase C<sub>18</sub> column (5–10  $\mu$ , 7.8  $\times$  250mm) using methanol–water gradients. The purified peptides were analyzed by electrospray mass spectrometry on a Hewlett-Packard HP-1100 LCMSD mass spectrometer and were fully characterized by 500 MHz <sup>1</sup>H NMR.

### Boc-Val-Lac-OBzl

Boc-Val-OH (0.65 g, 3 mmol) was dissolved in dichloromethane (DCM) (10 mL) and cooled in an ice bath with stirring. Lac-OBzl (L-lactic acid was converted to its benzyl ester with O-benzyl-N,N-dicyclohexyl isourea in refluxing tetrahydrofuran<sup>41</sup>; 0.54 g, 3 mmol) was added dropwise, followed by DCC (0.72 g, 3.5 mmol) and DMAP (0.15 g, 1.2 mmol). The reaction mixture was allowed to attain room temperature and stirred for 12 h. DCM was evaporated in vacuo. The residue was taken in ethyl acetate (10 mL) and the precipitated dicyclohexylurea (DCU) was filtered. The filtrate was washed with 1M sodium carbonate (3  $\times$  20 mL)

**Table I Crystal Data and Structure Refinement<sup>a</sup>**

Crystal	11-mer (1)	10-mer (2)	14-mer (3)
Empirical formula	(C <sub>56</sub> H <sub>100</sub> N <sub>10</sub> O <sub>15</sub> ) <sub>2</sub> · 5H <sub>2</sub> O	C <sub>53</sub> H <sub>95</sub> N <sub>9</sub> O <sub>14</sub>	C <sub>70</sub> H <sub>121</sub> N <sub>13</sub> O <sub>18</sub>
Formula weight	2386.92	1147.41	1432.80
Temperature °C	−50	20	19
Crystal system	Monoclinic	Triclinic	Triclinic
Space group	P2 <sub>1</sub>	P1	P1
Z	4	1	1
Unit cell dimensions	<i>a</i> = 21.352 (4) Å <i>b</i> = 9.592 (3) Å <i>c</i> = 34.178 (7) Å $\alpha$ = 90° $\beta$ = 93.250 (10)° $\gamma$ = 90°	<i>a</i> = 9.8060 (10) Å <i>b</i> = 11.348 (2) Å <i>c</i> = 15.468 (2) Å $\alpha$ = 107.370 (10)° $\beta$ = 100.170 (10)° $\gamma$ = 91.320 (10)°	<i>a</i> = 11.9080 (10) Å <i>b</i> = 13.041 (2) Å <i>c</i> = 15.211 (2) Å $\alpha$ = 85.380 (10)° $\beta$ = 85.960 (10)° $\gamma$ = 81.040 (10)°
Volume	6989 (3) Å <sup>3</sup>	1611.7 (4) Å <sup>3</sup>	2321.7 (5) Å <sup>3</sup>
Density (calculated)	1.134 mg/m <sup>3</sup>	1.182 mg/m <sup>3</sup>	1.025 mg/m <sup>3</sup>
Crystal size	1.4 × 0.28 × 0.15 mm	0.30 × 0.24 × 0.04 mm	0.44 × 0.30 × 0.11 mm
2 $\theta$ <sub>max</sub>	100°	116°	108°
Independent reflections	7775 ( <i>R</i> <sub>int</sub> = 0.0066)	4723 ( <i>R</i> <sub>int</sub> = 0.0000)	5512 ( <i>R</i> <sub>int</sub> = 0.0161)
Data/restraints/parameters	7767/0/1494	4723/3/685	5509/3/930
Final <i>R</i> indices [ <i>I</i> > 2 ( <i>I</i> )]	<i>R</i> <sub>1</sub> = 0.1004, <i>wR</i> <sub>2</sub> = 0.2544	<i>R</i> <sub>1</sub> = 0.0732, <i>wR</i> <sub>2</sub> = 0.1796	<i>R</i> <sub>1</sub> = 0.0799, <i>wR</i> <sub>2</sub> = 0.1697
Largest diff. Peak and hole	0.580 and −0.581 e Å <sup>−3</sup>	0.213 and −0.217 e Å <sup>−3</sup>	0.229 and −0.202 e Å <sup>−3</sup>

<sup>a</sup> X-ray diffraction data were measured on a Siemens P4s four-circle diffractometer with an oriented graphite crystal monochromator and CuK $\alpha$  radiation ( $\lambda$  = 1.54178 Å). Scan mode was  $\theta/2\theta$  and scan speed was constant 10 deg/min. A background measurement was made at both ends of every scan, each for 50% of the total scan time, and three reflections chosen as standards were monitored after every 97 measurements.

and brine (2 × 20 mL). The solution was dried over sodium sulfate and evaporated in vacuo. Boc–Val–Lac–OBzl was obtained as a light yellow gum (0.99 g, 2.6 mmol, 90%). 80 MHz <sup>1</sup>H NMR (CDCl<sub>3</sub>,  $\delta$  ppm) 0.94 (6H, m, Val C <sup>$\gamma$</sup> H<sub>3</sub>), 1.45 (9H, s, Boc CH<sub>3</sub>), 1.53 (3H, d, Lac C <sup>$\beta$</sup> H<sub>3</sub>), 2.25 (1H, m, Val C <sup>$\beta$</sup> H), 4.30 (1H, m, Val C <sup>$\alpha$</sup> H), 5.03 (1H, d, Val NH), 5.15 (m, 3H, OBzl–CH<sub>2</sub>/Lac C <sup>$\alpha$</sup> H), 7.31 (5H, m, phenyl).

### Boc–Val–Lac–OH

The amount of 0.95 g (2.5 mmol) of Boc–Val–Lac–OBzl was dissolved in 15 mL methanol containing two drops of glacial acetic acid. The amount of 0.15 g of 10% palladized charcoal was added and the suspension was subjected to hydrogenolysis. Twelve hours later palladized charcoal was filtered and the filtrate was evaporated in vacuo to yield a gum, which on standing yielded a white solid. (0.67 g, 2.3 mmol, 92%). 80 MHz <sup>1</sup>H NMR: (CDCl<sub>3</sub>,  $\delta$  ppm) 0.95 (6H, m, Val C <sup>$\gamma$</sup> H<sub>3</sub>), 1.45 (9H, s, Boc CH<sub>3</sub>), 1.5 (3H, d, Lac C <sup>$\beta$</sup> H<sub>3</sub>), 2.20 (1H, m, Val C <sup>$\beta$</sup> H), 4.25 (1H, m, Val C <sup>$\alpha$</sup> H), 5.05 (1H, q, Lac C <sup>$\alpha$</sup> H).

### Boc–Leu–Aib–Val–Ala–Leu–OMe

To 1.65 g (4 mmol) of Boc–Val–Ala–Leu–OMe<sup>42</sup> was added 15 mL of 98% formic acid, and the removal of Boc group was followed by TLC. After 10 h, formic acid was

evaporated. The residue was taken in water (15 mL) and the solution was adjusted to pH ~ 8 by addition of sodium carbonate, and extracted with ethyl acetate (3 × 20 mL). The extracts were pooled and dried over sodium sulfate and concentrated in vacuum to ~3 mL of highly viscous gum that yielded positive ninhydrin test. The tripeptide free base solution was added to an ice-cooled solution of Boc–Leu–Aib–OH<sup>43</sup> (1.3 g, 4 mmol) in N,N-dimethylformamide (DMF), followed by addition of 0.93 g (4.5 mmol) of DCC and 0.61 g (4.5 mmol) HOBt. The reaction mixture was stirred for 3 days at room temperature. fifteen milliliters of ethylacetate was added to the reaction mixture and DCU filtered off. The organic layer was washed with 1N HCl (3 × 20 mL), sodium carbonate (3 × 15 mL), and brine (2 × 20 mL). On subsequent drying over sodium sulfate and evaporation in vacuo, a white solid (1.6 g, 63%) was obtained, which was used directly for further chain elongation.

### Boc–Val–Lac–Leu–Aib–Val–Ala–Leu–OMe

The amount of 1.2 g (2.0 mmol) of Boc–Leu–Aib–Val–Ala–Leu–OMe was deprotected with 98% formic acid (8 mL) and worked up as reported above. This was coupled to 2 mmol (0.58 g) of Boc–Val–Lac–OH in DMF (5mL) using DCC (0.45 g, 2.2 mmol), HOBt (0.3 g, 2.2 mmol). After 3 days the reaction was worked up as described above to yield 1.2 g of a white solid. The peptide was characterized

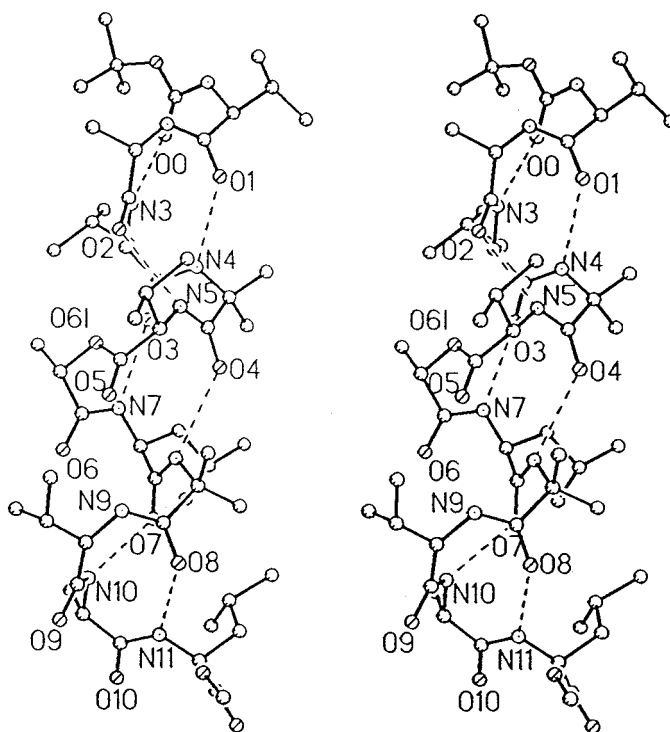


**FIGURE 1** Stereodiagram of the structure of Boc-Val-Ala-Leu-Aib-Val-Lac-Leu-Aib-Val-Ala-Leu-OMe (**1**). Note the ester O at O61. (Only one molecule of the two independent molecules is shown.)

by electrospray mass spectrometry ( $M_{Na^+}_{obs} = 807.7$ ;  $M_{calc} = 784.5$ ) and used without purification for further chain extension.

### Boc-Val-Ala-Leu-Aib-Val-Lac-Leu-Aib-Val-Ala-Leu-OMe (**1**)

The amount of 0.63 g (0.7 mmol) Boc-Val-Lac-Leu-Aib-Val-Ala-Leu-OMe was subjected to deprotection by 98 % formic acid (3 mL) and the isolated free base was added to a precooled solution of Boc-Val-Ala-Leu-Aib-OH<sup>42</sup> (0.38 g, 0.8 mmol) in 5 mL DMF, followed by 0.25 g (1.2 mmol) DCC and 0.16 g (1.2 mmol) of HOBT. After 4 days the reaction was worked up as described before. The final crude peptide **1** was obtained as a solid. The peptide was purified on a reverse phase C<sub>18</sub> MPLC column (40–60 $\mu$ ) using methanol water gradients (60–95%). The peptide was further purified by reverse phase HPLC C<sub>18</sub> (10 $\mu$ , 7.8  $\times$  250 mm) using a linear gradient of methanol water (65–95%). The peptide was homogeneous as analyzed on a reverse phase C<sub>18</sub> (5  $\mu$ ) column.  $M_{Na^+}_{obs} = 1175.7$ ;  $M_{calc} = 1152.7$ . Assignments of 500 MHz <sup>1</sup>H NMR are available.

### Boc-Val-Ala-Leu-Aib-Val-Lac-Leu-Aib-Val-Leu-OMe (**2**)

During the MPLC purification of **1**, a peptide fraction was collected which was shown to correspond to the sequence of

**2**.  $M_{Na^+}_{obs} = 1104.7$ ;  $M_{calc} = 1081.7$ . The crystal structure confirmed the constitution of the peptide.

### Boc-Val-Lac-Leu-OMe

The amount of 0.43 g (1.5 mmol) of Boc-Val-Lac-OH in 5 mL DMF was cooled in an ice bath and H-Leu-OMe [isolated from 0.55 g (3 mmol) of hydrochloride] was added followed by 0.4 g (2 mmol) DCC and 0.27 g (2 mmol) of HOBT. After stirring the reaction mixture for 2 days, the workup was done as described above. The compound was isolated as white solid (0.54 g, 1.3 mmol). 80 MHz <sup>1</sup>H NMR (CDCl<sub>3</sub>,  $\delta$  ppm) 0.95 (12H, m, Val C <sup>$\gamma$</sup> H<sub>3</sub>/Leu C <sup>$\delta$</sup> H<sub>3</sub>), 1.45 (9H, s, Boc CH<sub>3</sub>), 1.50 (3H, d, Lac C <sup>$\beta$</sup> H<sub>3</sub>), 1.54 (3H, m, Leu C <sup>$\beta$</sup> H<sub>2</sub>, C <sup>$\gamma$</sup> H), 2.25 (1H, m, Val C <sup>$\beta$</sup> H), 3.65 (3H, s, OCH<sub>3</sub>), 4.10 (1H, m, Val C <sup>$\alpha$</sup> H), 4.50 (1H, m, Leu C <sup>$\alpha$</sup> H), 4.80 (1H, d, Val NH) 5.15 (1H, q, Lac C <sup>$\alpha$</sup> H), 6.60 (1H, d, Leu NH).

### Boc-Val-Ala-Leu-Aib-Val-Lac-Leu-OMe

The amount of 0.54 g (1.3 mmol) of Boc-Val-Lac-Leu-OMe was deprotected using 5 mL of 98% formic acid and the free base, isolated as described above, was added to a precooled solution of 0.97 g (2 mmol) of Boc-Val-Ala-Leu-Aib-OH<sup>22</sup> in 5 mL DMF followed by 0.41 g (2 mmol) of DCC and 0.27 g (2 mmol) of HOBT. After 3 days the solution was worked up in the standard manner. The crude peptide was subjected to MPLC on a reverse phase C<sub>18</sub>

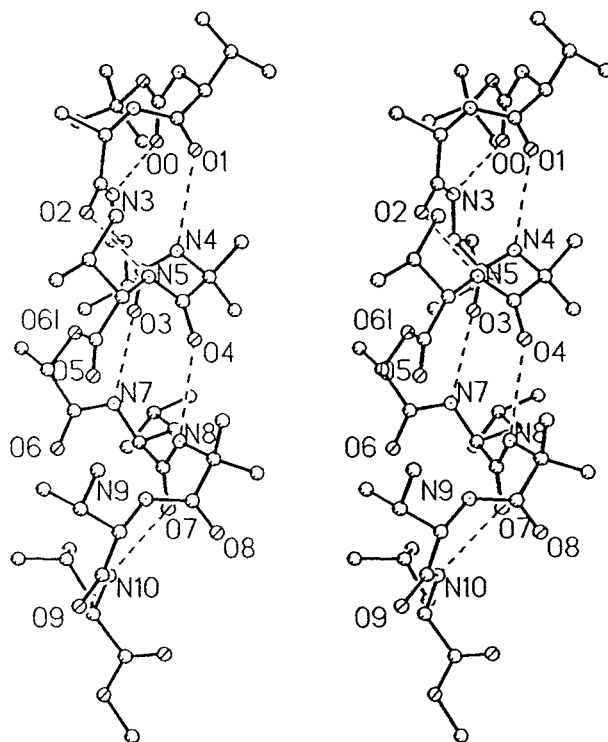


**FIGURE 2** Stereodiagram of the structure of Boc-Val-Ala-Leu-Aib-Val-Lac-Leu-Aib-Val-Leu-OMe (**2**). Note the ester O at O6l.

(40–60  $\mu$ ) column using methanol–water gradient. The MPLC purified peptide was characterized by electrospray mass spectrometry ( $M_{Na^+_{obs}} = 807.8$ ;  $M_{calc} = 784.5$ ) and was used directly for further chain elongation.

### Boc-Val-Ala-Leu-Aib-Val-Ala-Leu-Val-Ala-Leu-Aib-Val-Lac-Leu-OMe (**3**)

The amount of 0.23 g (0.3 mmol) of Boc-Val-Ala-Leu-Aib-Val-Ala-Leu-OH<sup>42</sup> was dissolved in 2 mL of DMF and the solution was cooled in an ice bath. To this solution a concentrated ethyl acetate solution of H-Val-Ala-Leu-Aib-Val-Lac-Leu-OMe, isolated from 0.15 g (0.2 mmol) of Boc-Val-Ala-Leu-Aib-Val-Lac-Leu-OMe upon deprotection with 2 mL of 98% formic acid, was added and the reaction was stirred for 4 days. The crude peptide isolated from this reaction mixture was purified by MPLC, followed by HPLC. The purified peptide was adjudged homogeneous on an analytical reverse phase C<sub>18</sub> column (5  $\mu$ ).  $M_{Na^+_{obs}} = 1458.5$ ;  $M_{calc} = 1435.9$ . 500 MHz <sup>1</sup>H NMR spectroscopy.

### Boc-Val-Ala-Leu-Aib-Val-Ala-Leu-Aib-Val-Ala-Leu-OMe (**4**)

This sequence is the Ala(6) analogue of peptide **1**, containing a normal peptide backbone. The peptide was synthesized by standard solution procedures and purified as described in the case of **1** and fully characterized by electro-

spray mass spectrometry ( $M_{Na^+_{obs}} = 1174.8$ ,  $M_{calc} = 1151.7$ ) and by 500 MHz <sup>1</sup>H NMR spectroscopy.

### X-Ray Crystallography

Crystals were grown by slow evaporation of solutions of the peptides in an organic solvent; **1** (11-residue peptide) from propanediol/water, **2** (10-residue peptide) from methanol/water, and **3** (14-residues) from methanol/dioxane/water. The peptide **1** cocrystallized with 5 water molecules. The crystals for **1** were very fragile and had to be stabilized by cooling to  $-50^\circ\text{C}$  for x-ray data collection. Very fragile crystals of **1** were also obtained from isopropanol/dimethylsulfoxide solution. These crystals did not yield sufficient number of x-ray reflections to determine the structure. The monoclinic unit cell had different dimensions than those obtained for the peptide **1** presented in this paper. Pertinent diffraction data are listed in Table I.

All the structures were solved by vector search procedures<sup>44</sup> using as model a portion of the Val-Ala-Leu-Aib-Val-Ala-Leu sequence in known peptide structures, followed by partial structure expansion with the tangent formula.<sup>45</sup> Full-matrix anisotropic least squares using  $F^2$  values were performed on the C, N, and O atoms. In the final cycles, H atoms were added in idealized positions and allowed to ride with the C or N atoms to which each was bonded. Cocrystallized solvent molecules occur in **1** and **3** crystals while there were none in **2**. Fractional coordinates for the C, N, and O atoms for the peptides **1–3** are deposited in the Cambridge Crystallographic Data Centre.

**Table II Backbone Torsion Angles<sup>a</sup> (deg) in the Depsipeptides 1 and 2<sup>b</sup>**

		1 A	1 B <sup>c</sup>	2
Boc	$\psi$	-166	-170	-173
	$\omega$	+180	-170	-169
Val1	$\phi$	-63	-63	-62
	$\psi$	-18	-25	-31
	$\omega$	+175	+180	-178
Ala2	$\phi$	-52	-51	-64
	$\psi$	-31	-35	-15
	$\omega$	+179	-179	+174
Leu3	$\phi$	-58	-60	-58
	$\psi$	-27	-19	-27
	$\omega$	+178	+174	+178
Aib4	$\phi$	-53	-49	-55
	$\psi$	-39	-42	-41
	$\omega$	-173	-172	-176
Val5	$\phi$	-79	-74	-64
	$\psi$	-35	-40	-44
	$\omega$	+175	+179	-176
Lac6	$\phi$	-64	-60	-69
	$\psi$	-42	-44	-36
	$\omega$	+177	+179	-179
Leu7	$\phi$	-59	-64	-78
	$\psi$	-45	-45	-36
	$\omega$	-172	-176	-164
Aib8	$\phi$	-52	-59	-60
	$\psi$	-44	-37	-35
	$\omega$	-174	-177	-171
Val9	$\phi$	-62	-72	-87
	$\psi$	-24	-47	-5
	$\omega$	+178	-174	-179
				Leu10
Ala10	$\phi$	-88	-76	-74
	$\psi$	-9	-39	+158
	$\omega$	-175	-169	-179
Leu11	$\phi$	-108	-117	
	$\psi$	-27	+25	
	$\omega$	-173	-178	

<sup>a</sup> Torsion angles for rotations about the bonds in the backbone as described in IUPAC-IUB Commission on Biochemical Nomenclature Biochemistry, 1970, Vol. 9, pp. 3471–3479.

<sup>b</sup> Peptide 2 differs from peptide 1 by omission of Ala10 from the 1.

<sup>c</sup> Two independent molecules in asymmetric unit of cell.

## NMR Spectroscopy

NMR studies were carried out on a Bruker DRX-500 spectrometer. All two-dimensional (2D) experiments were done in the phase sensitive mode using time proportional phase incrementation. Double quantum filtered correlated spectroscopy (DQF-COSY),<sup>46</sup> total correlated spectroscopy (TOCSY),<sup>47</sup> and rotating frame nuclear Overhauser effect spectroscopy (ROESY)<sup>48,49</sup> experiments were performed collecting 1K data points in f2 and 512 data points in f1

using a spectral width of 5500 Hz. Data were processed on a Silicon Graphics Indy work station using Bruker XWIN NMR software. Typically, a sine squared window function, phase shifted by  $\pi/2$  radians, was applied in both the dimensions. Data in f1 was zero-filled to 1K points. A spin lock mixing time of 300 ms was used in ROESY experiments and a 70 ms mixing time was used for TOCSY experiments. The sample concentration was  $\sim 3$  mM and the probe temperature was maintained at 300 K.

## Circular Dichroism

CD spectra were recorded on a JASCO J-715 spectropolarimeter. The instrument was calibrated with d(+)-10-camphorsulphonic acid. The path length used was 1 mm. The data were acquired in the wavelength scan mode, using 1 nm band width with a step size of 0.2 nm. Typically, 8 scans were acquired from 260 to 195 nm using 50 nm/min scan speed. The resulting data were baseline corrected and smoothened. The peptide concentrations were  $\sim 0.1$  mg/mL.

## RESULTS AND DISCUSSION

### Molecular Conformations in Crystals of Peptides 1 And 2

Figures 1 and 2 show the stereo diagrams of the crystallographically determined structures of the 11-residue peptide 1 and the 10-residue peptide 2. Peptide 1 crystallized with two independent molecules in the asymmetric unit that have very closely related backbone conformations. Consequently, the molecular conformation of only one of the crystallographically independent molecules is shown in Figure 1. Tables II and III summarize the backbone torsion angles and the observed hydrogen bonds in these peptides. The two independent molecules in the structures of peptide 1 and peptide 2 adopt mixed  $3_{10}/\alpha$ -helical conformations. The backbone torsion angles for residues 1–10 lie in the right handed region of  $\phi, \psi$  space ( $-60^\circ \pm 30^\circ, -30^\circ \pm 30^\circ$ ). Most notably, the Lac residue in the three determined peptide helices adopts  $\phi, \psi$  values very close to that expected for ideal helical structures [**1A** ( $-64^\circ, -42^\circ$ ): **1B** ( $-60^\circ, -40^\circ$ ): **2** ( $-69^\circ, -36^\circ$ )]. A comparison of the three peptide helices reveals small differences in the pattern of hydrogen bonds towards the C-terminus. For example, the N9  $\cdots$  O5 hydrogen bond is not observed in molecule **1A** and **2** (Table III).

Interestingly, the Lac residue resides comfortably in the center of the helix with the ester oxygen, O6Lac (O6l), nestling very close to the atom O3 of the Leu(3) CO group. The O6Lac  $\cdots$  O3 distance in all the three examples lies between 3.14 and 3.21 Å,

Table III Comparison of Hydrogen Bonds in Depsipeptides 1 and 2 with Normal Peptides 5 and 6

Type	Donor	Acceptor	N ··· O, Å 11-mer		Donor	Acceptor	N ··· O, Å 10-mer 2	N ··· O, Å 13-mer 5 <sup>b</sup>	N ··· O, Å 16-mer 6 <sup>c</sup>
			1 A	1 B <sup>a</sup>					
Head-to-tail	N1	O30 <sup>d</sup>	2.933		N1	O9	3.149		
	N21	O10 <sup>e</sup>		2.897					
	N2	W2 <sup>f</sup>	2.993		N2	O8	3.274		
4→1	N22	W1 <sup>f</sup>		3.123					
	N3	O0	3.144	3.031	N3	O0	2.974	2.848	3.078
	N4	O1	2.897	2.881	N4	O1	3.044	2.905	2.973
	N5	O2	2.985	3.058	N5	O2	2.974	3.210	3.296
5→1	[O6L	O3	3.209	3.152] <sup>g</sup>	[O6L	O3	3.138] <sup>g</sup>	3.488 <sup>h</sup>	3.047 <sup>i</sup>
	N7	O3	2.972	3.052	N7	O3	3.009	3.050	2.931
	N8	O4	3.005	2.971	N8	O4	2.979	2.958	3.197
	N9	O5	<sup>j</sup>	3.086	N9	O5	(3.82) <sup>k</sup>	3.200	3.113
4→1	N10	O7	2.909		N10	O7	3.154	3.064 <sup>l</sup>	2.999 <sup>m</sup>
5→1	N30	O26		3.118					
4→1	N11	O8	3.112						
5→1	N31	O27		2.840					
Water	W1	O9 <sup>n</sup>	2.957						
	W1	O11 <sup>o</sup>	2.874						
	W2	O30 <sup>p</sup>		2.950					
	W2	W3		2.873					
	W3	O29 <sup>p</sup>		2.655					
	W3	W4		2.581					
	W4	O29		2.704					
	W4	W5 <sup>q</sup>		2.878					
	W5	O28		3.069					

<sup>a</sup> Atom labels in 1B have 20 added to labels of equivalent atoms in 1A.

<sup>b</sup> Boc-Aib(Val-Ala-Leu-Aib)<sub>3</sub>-OMe (Ref. 67), a normal 13-residue peptide for comparison with depsipeptide.

<sup>c</sup> Boc-(Val-Ala-Leu-Aib)<sub>4</sub>OMe (Ref. 68) a normal 16-residue peptide for comparison.

<sup>d</sup>  $-x, \frac{1}{2} + y, -z$ .

<sup>e</sup>  $-1 + x, -1/2 + y, 1 - z$ .

<sup>f</sup>  $-1 + x, y, z$ .

<sup>g</sup> Not a hydrogen bond. Value represents distance between ester O and carbonyl O.

<sup>h</sup> N6 ··· O3 distance at transition between 4→1 and 5→1 hydrogen bonding. Both N6 and N7 are donors to O3.

<sup>i</sup> N6 ··· O2 distance at transition between 4→1 and 5→1 hydrogen bonding. Both N5 and N6 are donors to O2.

<sup>j</sup> No near acceptor atom.

<sup>k</sup> O5 is at too long a distance to be an acceptor atom.

<sup>l</sup> N10 ··· O6 distance at reverse transition between 5→1 and 4→1 hydrogen bonds.

<sup>m</sup> N10 ··· O6 distance. There is no transition to 4→1 type hydrogen bonds.

<sup>n</sup>  $-x, -1/2 + y, 1 - z$ .

<sup>o</sup>  $-x, -3/2 + y, 1 - z$ .

<sup>p</sup>  $1 - x, \frac{1}{2} + y, -z$ .

<sup>q</sup>  $1 - x, -1/2 + y, -z$ .

values remarkably similar to those obtained for N ··· O distances involved in hydrogen bonds in normal peptide helices. The 13-residue peptide 5, Boc-Aib(Val-Ala-Leu-Aib)<sub>3</sub>-OMe, and 16-residue peptide 6, Boc-(Val-Ala-Leu-Aib)<sub>4</sub>-OMe, have very similar sequences to 1-3 except that all residues are amino acids (Table III). It is curious that in peptide 5, the N6 ··· O3 distance has lengthened to 3.488 Å, a value considerably larger than found in any of the other peptides.

## Helix Assembly in Crystals

The helices in peptides 1 and 2 assemble into long columns held together by head-to-tail hydrogen bonds between free NH and CO groups at the N- and C-termini of helices, respectively. In peptide 2 there are two distinct NH ··· O hydrogen bonds (N1 ··· O9, N2 ··· O8) between adjacent helices in a column. The helices pack in a parallel fashion in the crystal, an inevitable requirement of the triclinic space group

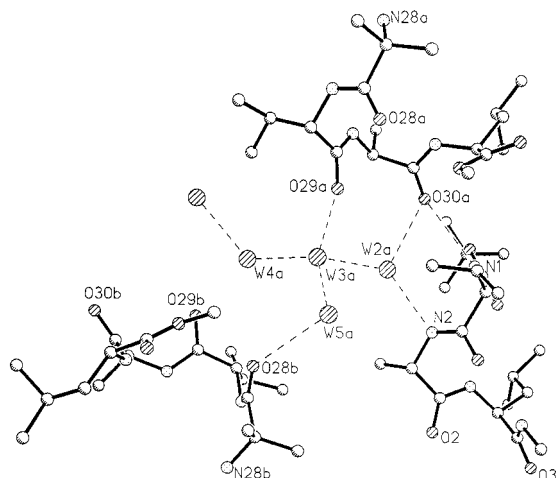


**FIGURE 3** A portion of three helices and the water structure in one of the head-to-tail regions of the crystal of peptide **1**. Shown are one direct N(1)H...O(30) bond and hydrogen bonds from four water molecules that bridge CO and NH groups from different helices.

(figure not shown). This mode of arrangement of cylindrical peptide molecules has been observed in several cases.<sup>33,34,50</sup>

The assembly and connections between the head and tail of peptide **1** are more complex. The two independent molecules alternate in a stack. The stacks assemble in an antiparallel motif. There is only one NH...O hydrogen bond between each pair of molecules, N(1)...O(30) at one head-to-tail junction and N(21)...O(10) at the other

**Table IV** Backbone Torsional Angles (deg) in Peptide **3**

Boc	$\psi$	-172		
	$\omega$	-173		
Val1	$\phi$	-56	Val8	-71
	$\psi$	-37		-44
	$\omega$	-177		180
Ala2	$\phi$	-55	Ala9	-58
	$\psi$	-34		-40
	$\omega$	180		-173
Leu3	$\phi$	-74	Leu10	-89
	$\psi$	-43		+4
	$\omega$	+174		-177
Aib4	$\phi$	-55	Aib11	+56
	$\psi$	-46		+36
	$\omega$	-177		+167
Val5	$\phi$	-63	Val12	-108
	$\psi$	-47		+51
	$\omega$	-178		+177
Ala6	$\phi$	-60	Lac13	-155
	$\psi$	-47		+147
	$\omega$	-176		+174
Leu7	$\phi$	-65	Leu14	-139
	$\psi$	-39		-47
	$\omega$	+179		-176

head-to-tail junction. Water molecules serve as additional bridges at the head-to-tail junctions, with as many as five molecules present in the crystal. The hydrogen-bonding scheme involving four independent water molecules at one of the head-to-tail regions is shown in Figure 3.

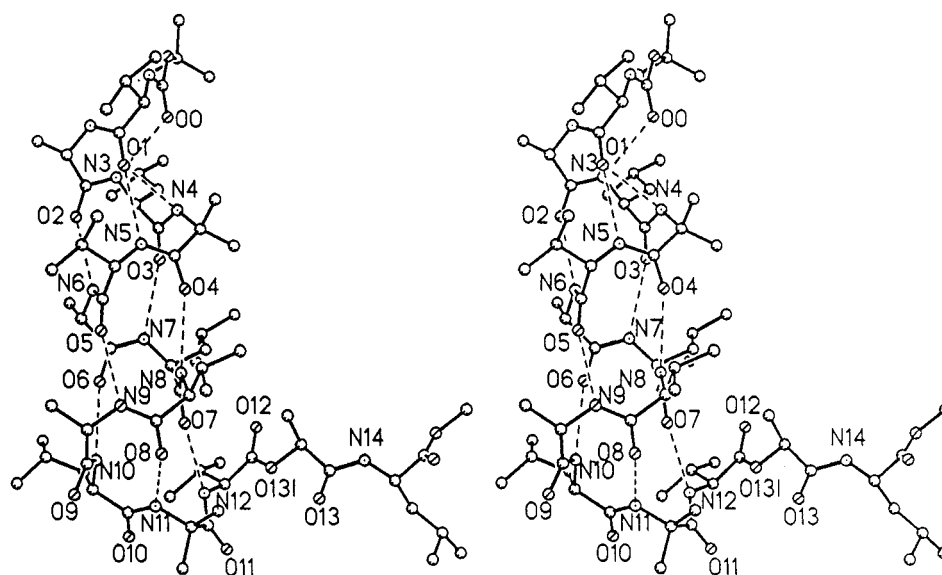


**FIGURE 4** Stereodiagram of molecular conformation of the 14-residue peptide Boc-Val-Ala-Leu-Aib-Val-Ala-Leu-Val-Ala-Leu-Aib-Val-Lac-Leu-OMe (**3**).



**Table V** Hydrogen Bonds in **3**

Type	Donor	Acceptor	N...O, Å
Head-to-tail	N1	O13 <sup>a</sup>	2.924
	N2	O11 <sup>a</sup>	2.876
4→1	N3	O0	3.020
	N4	O1	3.166 <sup>b</sup>
5→1	N5	O1	2.949
	N6	O2	2.987
	N7	O3	3.079
	N8	O4	3.077
	N9	O5	2.799
	N10	O6	3.225
Helix reversal			
4→1	N11	O8	3.119
6→1	N12	O7	2.969
Neighbor	N14	O9 <sup>c</sup>	2.870

<sup>a</sup> At  $x, -1 + y, +1 + z$ .<sup>b</sup> Very long H...O (2.68 Å).<sup>c</sup> At  $1 + x, y, z$ .

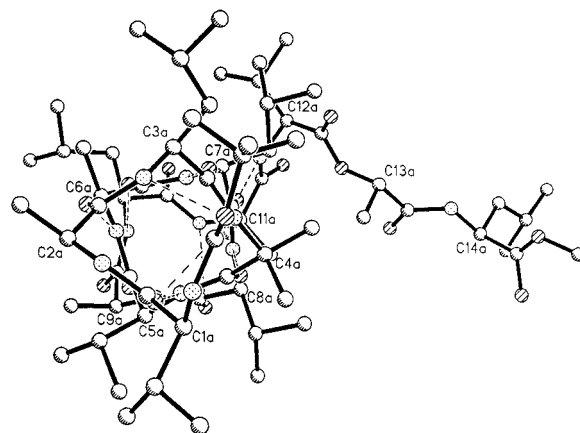
### Molecular Conformation of **3**

Figure 4 shows a stereo view of the molecular structure of **3** in crystals. The Lac residue was positioned at the C-terminus, residue 13, in order to promote helix termination as part of a strategy to construct helix-loop-helix motifs.<sup>51,52</sup> The crystal structure reveals that this expectation has indeed been realized with the four C-terminal residues Aib(11)–Leu(14) adopting backbone torsion angles, which lie well away from the right-handed helical region of  $\phi, \psi$  space. Backbone torsion angles and hydrogen bonds are summarized in Tables IV and V. Residues 1–10 adopt a helical conformation largely stabilized by 5 → 1 ( $\alpha$ ) hydrogen bonds, although the N-terminus is stabilized by 4 → 1 ( $3_{10}$ ) hydrogen bonds. Aib (11) adopts a left-handed helical ( $\alpha_L$ ) conformation with positive  $\phi, \psi$  values. This results in the termination of the helix formed by residues 1–10 with formation of a Schellman motif,<sup>53–55</sup> stabilized by a 6 → 1 hydrogen bond between Val(12) NH and Leu(7) CO groups. The helix termination motif also contains a second 4 → 1 hydrogen bond between Aib (11) NH and Val(8) CO groups (Table V), a feature often found to accompany the 6 → 1 hydrogen bond in the Schellman motif. The view in Figure 5 is directed down the axis of the helix and clearly illustrates the extension of the C-terminus away from the helix axis. Analysis of helix termination signals in protein structures<sup>56</sup> reveals that Pro, the only residue that lacks an NH group for internal hydrogen bonding, is most often found at the “T+2” position, where “T” is defined as the C-terminus residue that acts as the helix breaker by adopting  $\phi, \psi$  values in either the  $\alpha_L$  (left-

handed helical) or E (extended) region of Ramachandran space.<sup>57</sup> Interestingly, in peptide **3** the Lac 13 residue, which does not possess an NH group, occurs at the “T+2” position, with Aib(11) serving as the site of chiral reversal. The stereochemistry of the Schellman motif observed in peptide **3** is very close to that determined in a large number of crystalline peptides.<sup>58–62</sup> In most cases, the N...O distance for the 6 → 1 hydrogen bond is significantly shorter than that for the 4 → 1 hydrogen bond. The residue preceding the site of chiral reversal is also invariably found in the “bridge region” of the Ramachandran map, with  $\phi$  values  $\sim -80^\circ$  to  $\sim -100^\circ$  and  $\psi = -20^\circ$  to  $+20^\circ$ .<sup>59,61</sup>

### Molecular Packing in the Crystal

Despite the L-shaped extension at the end of the helical part of the backbone, the molecules of **3** still pack in a modified head-to-tail motif to form infinite columns of helices, as shown in Figure 6. For any one peptide molecule the extension of the L shape provides a N14...O9a hydrogen bond with the molecule to the side and a pair of hydrogen bonds, N1b...O13 and N2b...O11 to the molecule below, creating a sheet of nested L-shaped molecules. In space group P1, molecules repeat only by translation along each of the three axes of the cell. Hence the helix axes are all directed in the same direction, with consequent parallel packing. Figure 7, a view perpendicular to the one shown in Figure 6, illustrates hydrophobic channels that exist between the sheets of peptides. The channels are bounded by the *t*-Bu group, Ala9 side chain, and Leu10 side chain from three different molecules, and contain disordered solvent consisting of dioxane and possibly methanol molecules. The disorder has not been deciphered. It may be noted that hydrophobic channels containing

**FIGURE 5** View down the helix of **FIGURE 4**.

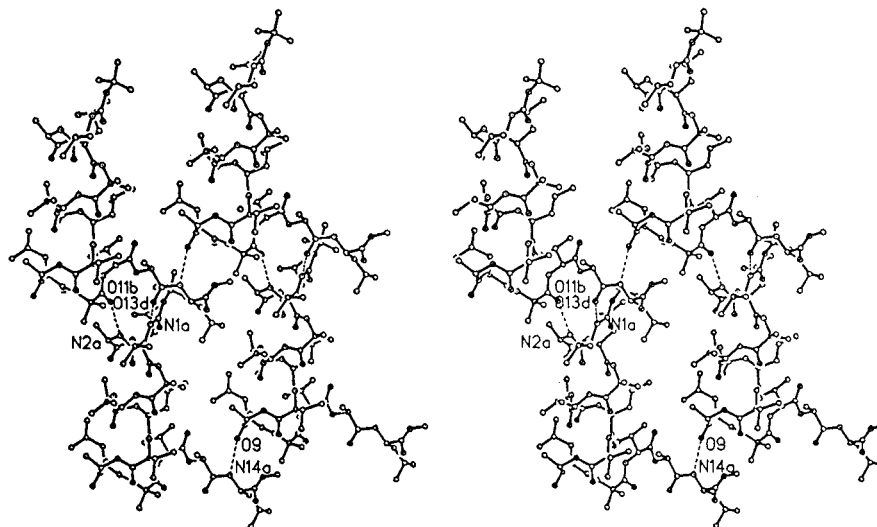


**FIGURE 6** Stereodiagram of four neighboring molecules of **3** forming a sheet structure by head-to-tail hydrogen bonds.

disordered solvent molecules have been observed in the crystal structures of cyclic and acyclic apolar peptides.<sup>63,64</sup>

### Solution Conformations of Peptide **1**

The observation that peptides **1** and **2** adopt helical conformations accommodating the ester unit in the central segment prompted us to investigate whether the observed structure was a consequence of the facile packing of cylindrical peptides into single crystals. Solution NMR and CD studies were therefore undertaken for peptide **1** and the corresponding L-Ala(6) analogue (the all amide analogue), Boc-Val-Ala-Leu-Aib-Val-Ala-Leu-Aib-Val-Ala-Leu-OMe, **4**. Figure 8 shows the comparison of CD spectra for

peptides **1** and **4** in 2,2,2-trifluoroethanol (TFE). Very similar spectra were also obtained in methanol (data not shown). Peptide **4** exhibits the canonical spectrum expected for a peptide helix consisting of about 3–4 helical turns; the exciton split  $\pi-\pi^*$  transition (190 nm and 205 nm) and the broad  $n-\pi^*$  band (220 nm) are characteristic helical features.<sup>65</sup> The Lac containing peptide **1** exhibits very similar spectral features, although the band intensities are somewhat diminished.

Proton NMR studies at 500 MHz of peptide **4** (the all amide analogue of **1**) in deuterated dimethyl sulfoxide (DMSO- $d_6$ ) solution permitted complete assignment of all resonances. Sequential  $N_iH \leftrightarrow N_{i+1}H$  NOEs could be traced over the entire length of the peptide, confirming a continuous helical conformation

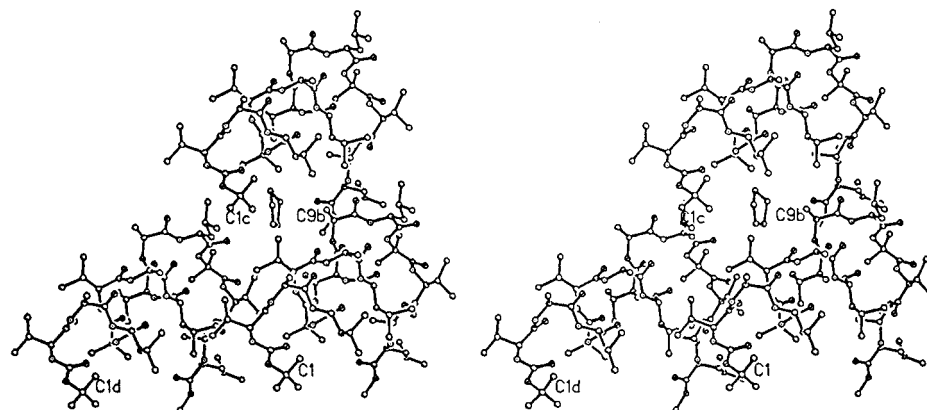


**FIGURE 7** Stereodiagram of a hydrophobic channel formed by three molecules of **3**. The channel is formed between the sheets. A possible solvent molecule is shown.

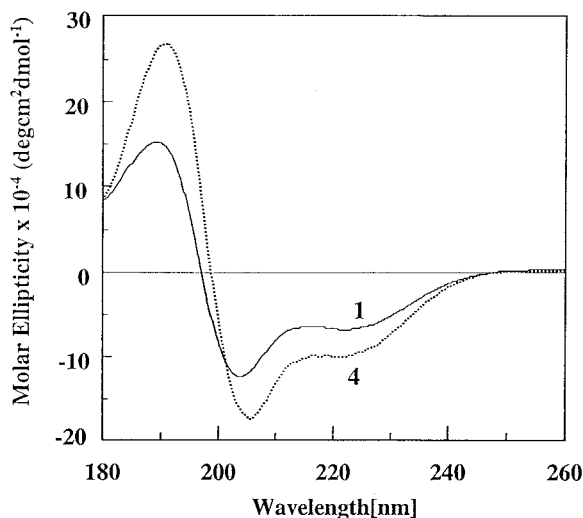


**FIGURE 8** Far-uv CD spectra of peptide **1**, Boc-Val-Ala-Leu-Aib-Val-Lac-Leu-Aib-Val-Ala-Leu-OMe and its all-amide analogue **4** (Boc-Val-Ala-Leu-Aib-Val-Ala-Leu-Aib-Val-Ala-Leu-OMe) in TFE (300 K).

(data not shown). In deuterated chloroform ( $\text{CDCl}_3$ ) solution there was considerable spectral overlap of NH resonances.

The 500 MHz  $^1\text{H}$  NMR spectrum of peptide **1** in  $\text{CDCl}_3$  was extremely well resolved, facilitating unambiguous assignments of all the backbone and side-chain protons using a combination of DQF-COSY and ROESY experiments. Figure 9 and 10 show partial ROESY spectra illustrating backbone  $\text{N}_i\text{H} \leftrightarrow \text{N}_{i+1}\text{H}$  ( $d_{\text{NN}}$ ) and  $\text{C}_i^\alpha\text{H} \leftrightarrow \text{N}_i\text{H}$  NOEs in peptide **1**. Sequential  $d_{\text{NN}}$  connectivities characteristic of a helical conformation can be traced for the segments 1–5 and 7–11 (Figure 9). Helical structures in peptide sequences give rise to characteristic medium-range NOEs between the  $\text{C}^\alpha\text{H}$  of residue  $i$  and NH of residues  $i+2/i+3/i+4$ . Intense  $d^{\alpha\text{N}}(i, i+3)$  NOEs are diagnostic of both  $3_{10}$ - and  $\alpha$ -helical conformations in peptide sequences.<sup>66</sup> From Figure 10 it is clear that several short  $\text{C}_i^\alpha\text{H} \leftrightarrow \text{N}_j\text{H}$  ( $j = 2-4$ ) are observed providing firm evidence in favor of helical  $\phi, \psi$  values throughout the sequence of **1**. Most notably, the boxed NOEs in Figure 10 indicate the NOEs diagnostic of helical conformations for the 3–9 segment, which contains

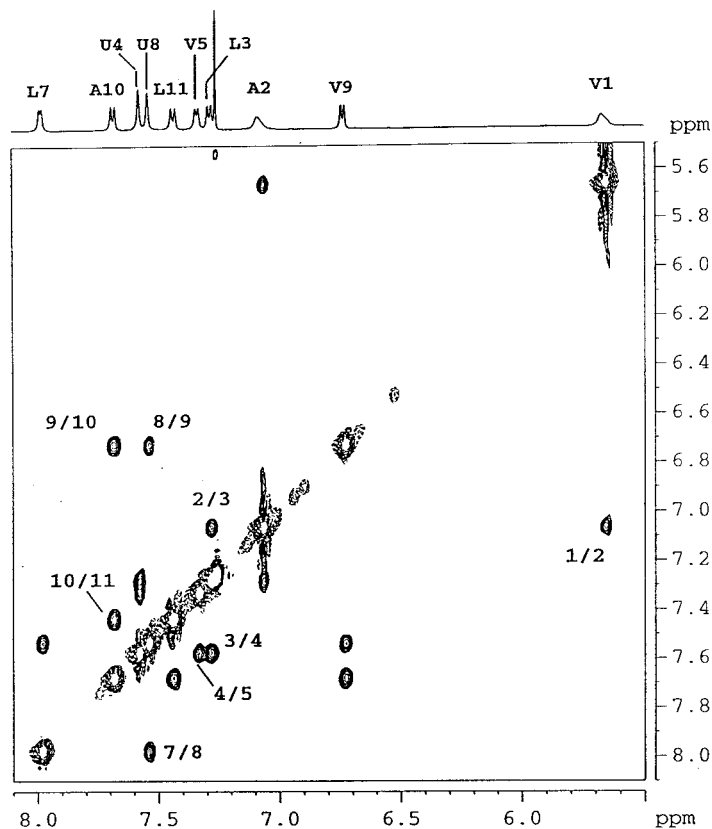


**FIGURE 9** Partial 500 MHz  $^1\text{H}$  ROESY spectrum of **1** (Boc-Val-Ala-Leu-Aib-Val-Lac-Leu-Aib-Val-Ala-Leu-OMe) in  $\text{CDCl}_3$  illustrating  $\text{N}_i\text{H} \leftrightarrow \text{N}_{i+1}\text{H}$  NOEs. Cross peaks are marked by residue numbers. In the projected 1D spectrum on top of the 2D figure, one letter codes for amino acids have been used (A = Ala, L = Leu, V = Val, U = Aib).

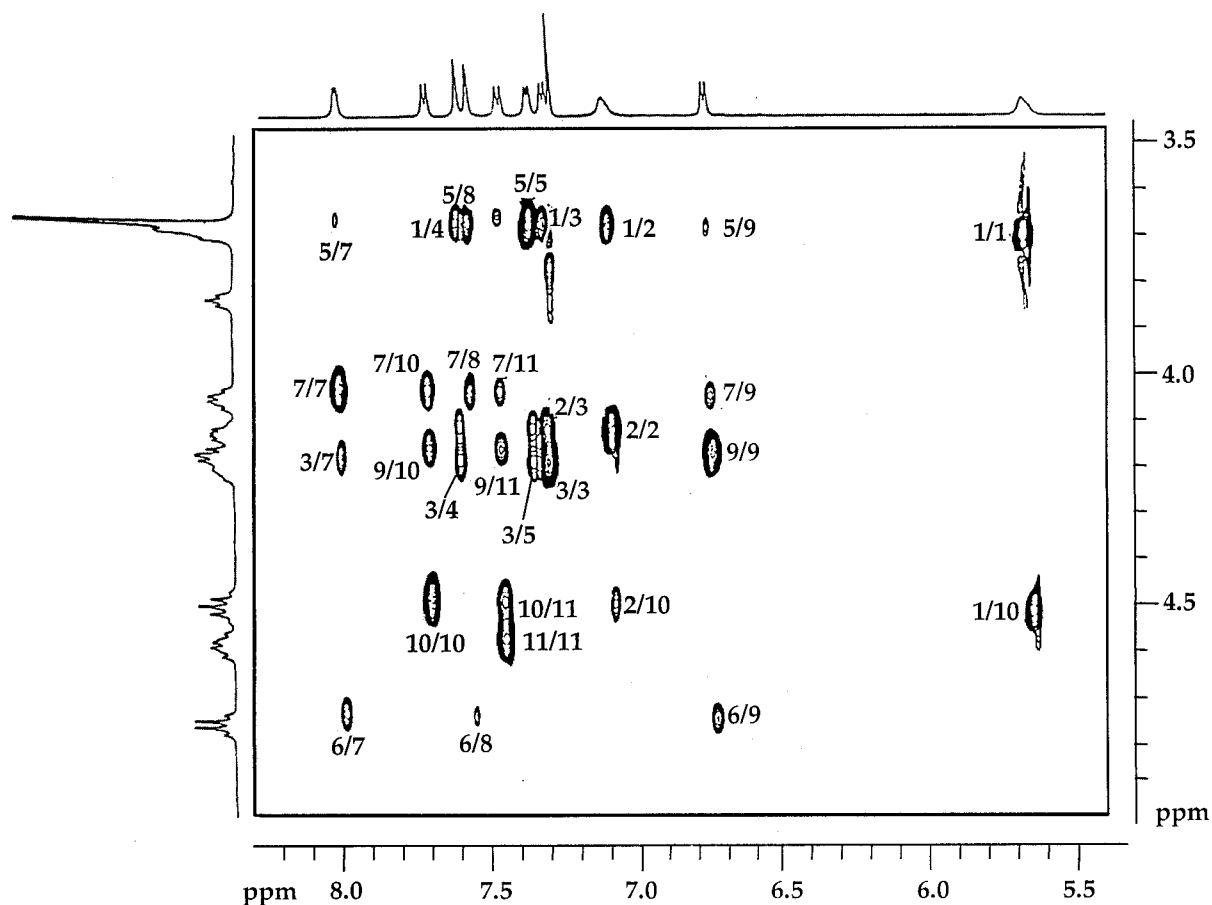


**FIGURE 10** Partial 500 MHz  $^1\text{H}$  ROESY spectrum of **1** (Boc-Val-Ala-Leu-Aib-Val-Lac-Leu-Aib-Val-Ala-Leu-OMe) in  $\text{CDCl}_3$  showing  $\text{C}^\alpha\text{H} \leftrightarrow \text{NH}$  NOEs. NOEs between groups from the N- and C-terminal sides of Lac(6) are highlighted by boxes enclosing them. Residue numbers are used to annotate the cross peaks.

the Lac residue (at position 6). The observation of these NOEs suggests a major population of solution conformations that closely resemble that observed in the crystal, accommodating the Lac residue at a central position in the helix.

Two NOEs observed in Figure 10,  $\text{NH}(1) \leftrightarrow \text{C}^\alpha\text{H}(10)$  and  $\text{NH}(2) \leftrightarrow \text{C}^\alpha\text{H}(10)$  may be assigned to intermolecular interactions arising from head to tail aggregation of cylindrical, helical structures. Such modes of helix association have been postulated in solution<sup>69</sup> and extensively observed in solid state.<sup>50</sup>

## CONCLUSIONS

The results presented in this paper provide definitive structural evidence that  $\alpha$ -hydroxy acids can be accommodated at central positions in peptide helices. The integrity of the helical conformations remains intact despite the abolition of a single intramolecular  $\text{CO} \cdots \text{NH}$  hydrogen bond. The observation that the

ester O in the lactic acid residue resides comfortably in proximity to a CO group with an  $\text{O} \cdots \text{O}$  distance of  $\sim 3.1 \text{ \AA}$  is intriguing. The possibility that specific electronic effects stabilize such an orientation merits further investigation. The influence of critical backbone hydrogen bonds on structure and function in peptides and proteins has been probed using amide to ester replacements. In the case of Eglin C, the C-terminus Gly residue has been replaced by  $\alpha$ -hydroxy acetamide resulting in a destabilization of about  $2.7 \text{ Kcal mol}^{-1}$ .<sup>70</sup> In a recent study, the Val(1)-Gly(2) peptide bond in gramicidin A has been replaced by an ester linkage, a substitution anticipated to perturb a key intermolecular hydrogen bond involved in dimer formation. The substitution has little effect on dimer stability, but profoundly effects channel lifetimes and stability.<sup>71</sup>

Incisive analyses of the hydrogen bond contribution in  $\alpha$ -helices in proteins using unnatural amino acid mutagenesis to insert  $\alpha$ -hydroxyacids have suggested that substitution of amide groups by an ester

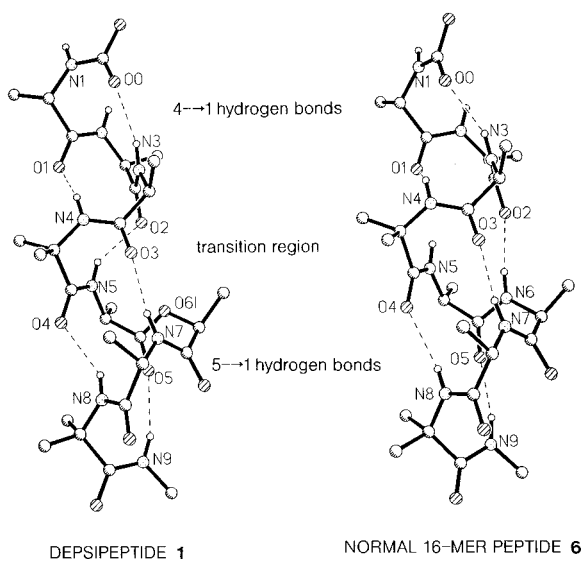


**FIGURE 11** The similarity in the transition region between 4 → 1 and 5 → 1 hydrogen bonds in comparable fragments of the depsipeptide **1** and the normal 16-mer peptide **6**. The ether linkage in **1** is labeled O6I while the normal amide linkage in **6** is labeled N6.

results in a destabilization of  $0.7\text{--}1\text{ kcal mol}^{-1}$ , when only one hydrogen bond is perturbed.<sup>30</sup> Somewhat greater destabilization ( $1.5\text{--}2.5\text{ kcal mol}^{-1}$ ) is observed in internal  $\beta$ -sheets.<sup>29</sup> Schultz and co-workers have suggested that decreased energetic contribution of hydrogen bonds in helices as compared to those in  $\beta$ -sheets “may be a result of increased solvent accessibility to backbone or electrostatic effects associated with the backbone.”<sup>30</sup> It is pertinent to note that replacement of an amide NH by an ester O in the center of an  $\alpha$ -helix can be compensated by a small conformational adjustment to a  $3_{10}/\alpha$ -helical structure in the vicinity of the “mutated residue.” Such a transition between 4 → 1 and 5 → 1 backbone hydrogen bonds is indeed observed in both crystallographically independent molecules peptide **1** and peptide **2** centered around position 6, which is the site of lactic acid insertion (Table III). A comparison of the 4 → 1 to 5 → 1 transition in the depsipeptide **1** and the 16-mer normal peptide is shown in Figure 11. This type of structural adjustment would result in a very small energy penalty when Lac residues are introduced into helices.

After this paper was submitted to *Biopolymers*, the structure of the depsipeptide Boc-(Leu-Leu-Ala)<sub>2</sub>-(Leu-Leu-Lac)<sub>3</sub>-OEt was published in *Biopolymers*.<sup>72</sup> This molecule also forms a mixed  $3_{10}/\alpha$ -helix with small distortions at Lac9 in the middle of the sequence.

In the 14-residue peptide the location of the Lac residue at position 13 results in a structure that reveals

helix termination at position 11, which is occupied by the achiral Aib residue. It is noteworthy that a continuous helix has been demonstrated in the crystals of a related 15-residue peptide, Boc-Val-Ala-Leu-Aib-Val-Ala-Leu-Val-Ala-Leu-Aib-Val-Ala-Leu-Aib-OMe.<sup>68</sup> It would appear that the propensity of Aib11 to switch helical sense and nucleate the terminating Schellman motif is determined by the loss of hydrogen bonding potential at the C-terminus, presumably as a consequence of the location of the Lac residue. It is notable that formation of the Schellman motif provides a strong 6 → 1 hydrogen bond, a feature that may be energetically advantageous when the chain of continuous helical hydrogen bonds is interrupted by the Lac residue. The present studies provide a clear high resolution glimpse of the effects of  $\alpha$ -hydroxy acid substitution in peptide helices.

This research was partially supported by the program on “Drug and Molecular Design” of the Department of Biotechnology, Government of India, by the National Institutes of Health Grant GM30902 and the Office of Naval Research, Washington, D.C. The NMR spectra were recorded at the Sophisticated Instruments Facility, Indian Institute of Science, Bangalore.

## REFERENCES

- Baker, E. N.; Hubbard, R. E. *Prog Biophys Mol Biol* 1984, 44, 97–179.
- Stickle, D. F.; Presta, L. G.; Dill, K. A.; Rose, G. D. *J Mol Biol* 1992, 226, 1143–1159.
- Richardson, J. S. *Adv Protein Chem* 1981, 34, 167–339.
- Karle, I. L. In *The Peptides*; Gross, E., Meienhofer, J. Eds.; Academic: New York, 1981, Vol 4, pp 1–54.
- Toniolo, C. *CRC Crit Rev Biochem* 1980, 9, 1–44.
- Pauling, L.; Corey, R. B.; Branson, H. R. *Proc Natl Acad Sci USA* 1951, 37, 205–211.
- Pauling, L.; Corey, R. B. *Proc Natl Acad Sci USA* 1951, 37, 251–256.
- Karle, I. L.; Karle, J. *Acta Cryst* 1963, 16, 969–975.
- Zalkin, A.; Forrester, J. D.; Templeton, D. H. *J Am Chem Soc* 1966, 88, 1810–1814.
- Kakudo, M.; Sasada, Y.; Katsube, S.; Sakakibara, S.; Akabori, S. In *Aspects of Protein Structure*; Ramachandran, G. N., Ed.; Academic: London, 1963; p 69.
- Venkatachalam, C. M. *Biopolymers* 1968, 6, 1425–1436.
- Chandrasekaran, R.; Lakshminarayanan, A. V.; Pandya, U. V.; Ramachandran, G. N. *Biochim Biophys Acta* 1973, 303, 14–27.
- Jeffrey, G. A.; Saenger, W. *Hydrogen Bonding in Biological Molecules*; Springer-Verlag: New York, 1991.
- Dill, K. A. *Biochemistry* 1990, 29, 7133–7155.
- Honig, B.; Yang, A. S. *Adv Protein Chem* 1995, 46, 27–58.

16. Murphy, K. P.; Gill, S. J. *J. Mol. Biol.* 1991, 222, 699–709.
17. Wiberg, K. B.; Laidig, K. E. *J. Am. Chem. Soc.* 1987, 109, 5935–5943.
18. Ingwall, R. T.; Goodman, M. *Macromolecules* 1974, 7, 598–605.
19. Boussard, C.; Marraud, M.; Neel, J.; Maigret, B.; Aubry, A. *Biopolymers* 1977, 16, 1033–1052.
20. Valle, G.; Bardi, R.; Piazzesi, A. M.; Crisma, M.; Toniolo, C.; Cavicchioni, G.; Uma, K.; Balaram, P. *Biopolymers* 1991, 31, 1669–1676.
21. Arad, O.; Goodman, M. *Biopolymers* 1990, 39, 1633–1649.
22. Katakai, R.; Goodman, M. *Macromolecules* 1982, 15, 25–30.
23. Wouters, G.; Katakai, R.; Becktel, W. J.; Goodman, M. *Macromolecules* 1982, 15, 31–35.
24. Gallo, E. A.; Gellman, S. H. *J. Am. Chem. Soc.* 1993, 115, 9774–9775.
25. Haque, T. S.; Little, J. C.; Gellman, S. H. *J. Am. Chem. Soc.* 1994, 116, 4105–4106.
26. Haque, T. S.; Little, J. C.; Gellman, S. H. *J. Am. Chem. Soc.* 1996, 118, 6975–6985.
27. Ellman, J. A.; Mendel, D.; Schultz, P. G. *Science* 1992, 255, 197–200.
28. Shin, I.; Ting, A. Y.; Schultz, P. G. *J. Am. Chem. Soc.* 1997, 119, 12667–12668.
29. Chapman, E.; Thorson, J. S.; Schultz, P. G. *J. Am. Chem. Soc.* 1997, 119, 7151–7152.
30. Koh, J. T.; Cornish, V. W.; Schultz, P. G. *Biochemistry* 1997, 36, 11314–11322.
31. Groeger, C.; Wenzel, H. R.; Tschesche, H. *Int. J. Peptide Protein Res.* 1994, 44, 166–172.
32. Lu, W.; Qasim, M. A.; Laskowski, M., Jr.; Kent, S. B. H. *Biochemistry* 1997, 36, 673–679.
33. Karle, I. L.; Balaram, P. *Biochemistry* 1990, 29, 6747–6756.
34. Karle, I. L. *Acc. Chem. Res.* 1999, 32, 693–701.
35. Balaram, P. *Curr. Opin. Struct. Biol.* 1992, 24, 845–851.
36. Toniolo, C.; Benedetti, E. *Macromolecules* 1991, 24, 4004.
37. Toniolo, C.; Benedetti, E. *Trends Biochem. Sci.* 1991, 16, 350–353.
38. Toniolo, C.; Benedetti, E. *ISI Atlas Sci. Biochem.* 1988, 1, 225–230.
39. Bodanszky, M. *Principle of Peptide Synthesis*; Springer-Verlag: Heidelberg, 1984.
40. Gilon, C.; Klausner, Y.; Hassner, A. *Tetrahedron Lett.* 1979, 40, 3811–3814.
41. Schmidt, E.; Dabritz, E.; Thulke, K.; Grassman, E. *Justus Liebig's Ann. Chem.* 1965, 685, 161–166.
42. Uma, K. Ph.D. Thesis, Indian Institute of Science, Bangalore, 1992.
43. Balaram, H.; Sukumar, M.; Balaram, P. *Biopolymers* 1986, 25, 2209–2223.
44. Egert, E.; Sheldrick, G. M. *Acta Cryst.* 1985, A41, 262–268.
45. Karle, J. *Acta Cryst.* 1968, B24, 182–186.
46. Piantini, U.; Sorensen, O. W.; Ernst, R. R. *J. Am. Chem. Soc.* 1982, 104, 6800–6801.
47. Braunschweiler, L.; Ernst, R. R. *J. Magn. Reson.* 1983, 53, 521–528.
48. Bax, A.; Davis, D. G. *J. Magn. Reson.* 1985, 63, 207–213.
49. Bothner-By, A. A.; Stephens, R. L.; Lee, J.; Warren, C. D.; Jeanloz, R. W. *J. Am. Chem. Soc.* 1984, 106, 811–812.
50. Karle, I. L. *Acta Cryst.* 1992, B48, 341–356.
51. Balaram, P. *Pure Appl. Chem.* 1992, 64, 1061–1067.
52. Kaul, R. K.; Balaram, P. *Bioorg. Med. Chem.* 1999, 7, 105–117.
53. Schellman, C. In *Protein Folding*; Jaenicke, R., Ed.; Elsevier/North Holland Medical Press: Amsterdam, 1980; pp 53–61.
54. Nagarajaram, H. A.; Sowdhamini, R.; Ramakrishnan, C.; Balaram, P. *FEBS Lett.* 1993, 321, 79–83.
55. Aurora, R.; Srinivasan, R.; Rose, G. D. *Science* 1994, 264, 1126–1130.
56. Gunasekaran, K.; Nagarajaram, H. A.; Ramakrishnan, C.; Balaram, P. *J. Mol. Biol.* 1998, 215, 917–932.
57. Ramachandran, G. N.; Ramakrishnan, C.; Sasisekharan, V. *J. Mol. Biol.* 1963, 7, 95–99.
58. Karle, I. L.; Flippen-Anderson, J. L.; Uma, K.; Balaram, P. *Int. J. Peptide Protein Res.* 1993, 42, 401–410.
59. Datta, S.; Shamala, N.; Banerjee, A.; Pramanik, A.; Bhattacharjya, S.; Balaram, P. *J. Am. Chem. Soc.* 1997, 119, 9246–9251.
60. Banerjee, A.; Datta, S.; Pramanik, A.; Shamala, N.; Balaram, P. *J. Am. Chem. Soc.* 1996, 118, 9477–9483.
61. Datta, S.; Uma, M. V.; Shamala, N.; Balaram, P. *Biopolymers* 1999, 50, 13–22.
62. Karle, I. L.; Das, C.; Balaram, P. *Proc. Natl. Acad. Sci. USA* 2000, 97, 3034–3037.
63. Karle, I. L. *J. Am. Chem. Soc.* 1977, 99, 5152–5157.
64. Rao, C. P.; Shamala, N.; Nagaraj, R.; Rao, C. N. R.; Balaram, P. *Biochem. Biophys. Res. Commun.* 1981, 103, 898–904.
65. Woody, R. W. In *The Peptides*; Udenfriend, S.; Meienhofer, J.; Hruby, V. J., Eds.; Academic: New York, 1985; Vol 7, pp 15–114.
66. Wüthrich, K. *NMR of Proteins and Nucleic Acids*; Wiley: New York, 1986.
67. Karle, I. L.; Flippen-Anderson, J. L.; Uma, K.; Balaram, P. *Biochemistry* 1989, 28, 6696–6701.
68. Karle, I. L.; Flippen-Anderson, J. L.; Uma, K.; Sukumar, M.; Balaram, P. *J. Am. Chem. Soc.* 1990, 112, 9350–9356.
69. Banerjee, A.; Raghothama, S.; Balaram, P. *J. Chem. Soc. Perkin 2*, 1977, 2087–2094.
70. Lu, W.-Y.; Starovasnik, M. A.; Dwyer, J. J.; Kossiakof, A. A.; Kent, S. B. H.; Lui, W. *Biochemistry* 2000, 39, 3575–3584.
71. Jude, A. R.; Providence, L. L.; Schmutzer, S. E.; Shobana, S.; Greathouse, D. V.; Anderson, O. S.; Koeppe, R. E., II. *Biochemistry* 2001, in press.
72. Ohyama, T.; Oku, H.; Hiroki, A.; Maekawa, Y.; Yoshida, M.; Katakai, R. *Biopolymers* 2000, 54, 375–378.